Chapter 3
Problem formulation

_____

3.1 Introduction

This chapter shows how the objective function is formulated and the physical model to be analysed is described. The open and direct solar thermal Brayton cycle will be used in the analysis.

Firstly, the different possibilities of arrangements of components in the solar thermal Brayton cycle are identified to show the uniqueness of the open and direct solar thermal Brayton cycle. The entropy generation rate in each of the heat exchangers and components in the system is identified. The total entropy generation rate for the whole system can be found when adding the entropy generation rates of each component in the system. The net power output of the system can be linked with the total entropy generation rate by doing an exergy analysis for the whole system.

In this chapter, the geometries of the components to be optimised are shown. The objective function is written in terms of the geometry variables. For the objective function, the constraints and assumptions are also listed. The assumption of steady-state is used as was mentioned in Chapter 1.

3.2 Different cases

When a heat source, $\dot{Q}_{net}$, is available (with the use of solar concentration), mechanical power can be generated by means of the solar thermal Brayton cycle. In the following figures, $\dot{Q}_{net}$ represents the net absorbed heat rate by the working fluid in the receiver, or the intercepted power minus the heat loss rate.

For the solar thermal Brayton cycle, there are a few different arrangements of the components to establish a working system. Four cases are shown here, so that the uniqueness of the open and direct solar thermal Brayton cycle can be clear. From the literature, it is concluded that the Brayton cycle has high thermal efficiencies and low compressor pressure ratios when a recuperator is used. A recuperator is used in each of the considered cases. Multistaging is

disregarded, but can be considered for further studies. The benefits and disadvantages of using a direct or indirect system are available in the literature (Stine and Harrigan, 1985).

Case 2 will be used for the analysis. It is the simplest case and has the least components, which means it might also be the cheapest. Minimisation of the entropy generation rate for maximum net power output in the other three cases is recommended for further study to be compared with this work.

3.2.1 Case 1

Figure 3.1 shows a direct system with a closed cycle. The power cycle is closed, meaning that the working fluid cycles through the system and does not exit the system. The radiator cools down the working fluid before it is compressed. The system is also direct – there is no secondary loop which captures the sun's heat and also no heat exchanger to transfer heat between two different working fluids. The solar collector uses the concentrated power of the sun to heat up the working fluid directly.
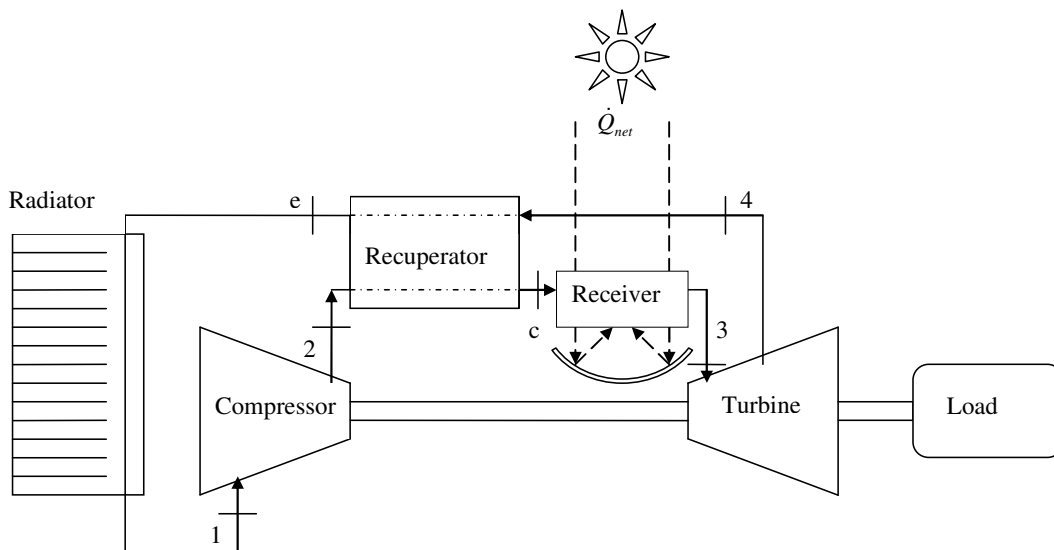

Figure 3.1 Case 1: Direct system, closed cycle.

3.2.2 Case 2

Figure 3.2 shows a direct system with an open cycle (the cycle to be used for this study). The system is open, which means that the working fluid (air) can enter and exit the cycle from and to the surroundings. There is no radiator required, since the air coming in from the surroundings is at the surrounding temperature. It is important that there is a natural flow of air through the system, so that the warm air from the exhaust does not go into the inlet. The system is also direct – there is no secondary loop which captures the sun's heat and also no heat exchanger to

transfer heat between two different working fluids. The solar collector heats up the air directly, using the sun's concentrated power.

3.2.3 Case 3

Figure 3.3 shows an indirect system with a closed cycle. The system is closed, meaning that the working fluid cycles through the system and does not exit the system. The radiator cools down the working fluid before it is compressed. The system is indirect – a secondary loop captures the sun's heat and a heat exchanger transfers heat between the two different fluids.
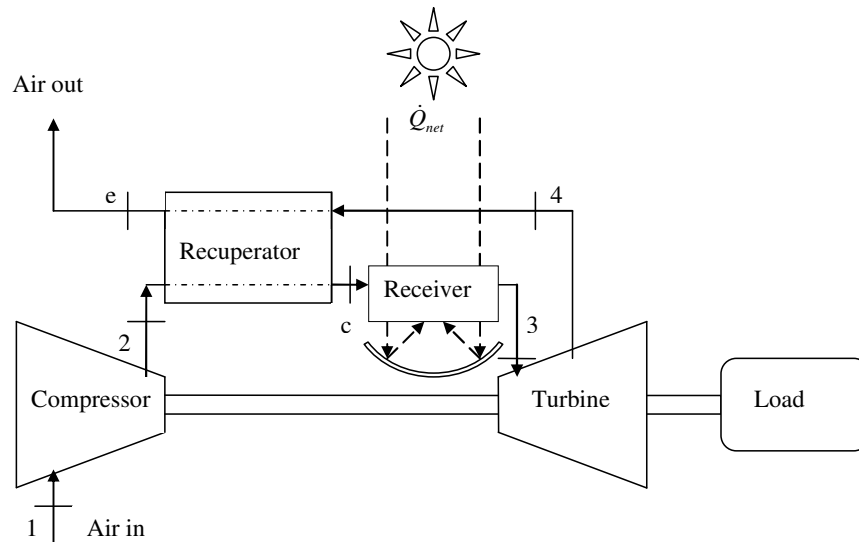

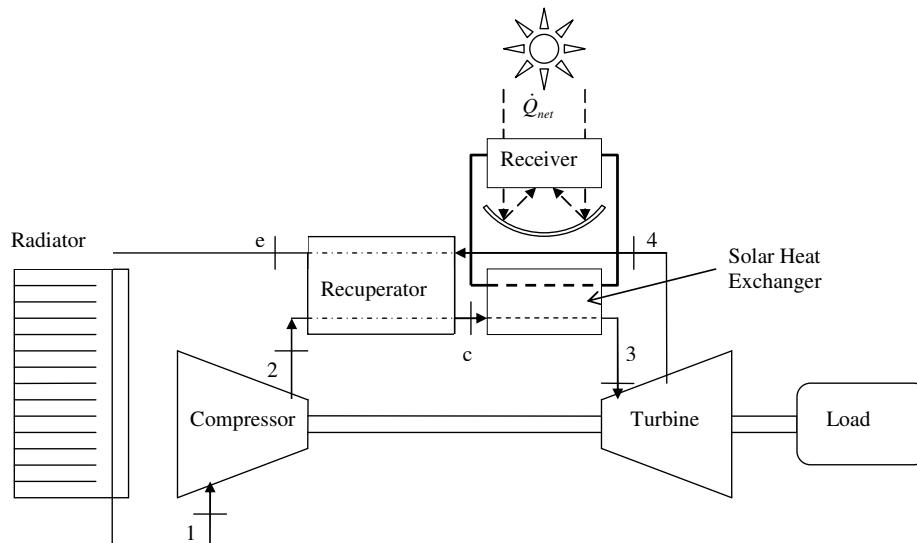**Figure 3.2 Case 2: Direct system, open cycle.**

Figure 3.3 Case 3: Indirect system, closed cycle.

3.2.4 Case 4

Figure 3.4 shows an indirect system with an open cycle. The system is open, which means that the air can enter and exit the cycle from and to the surroundings. There is no radiator required, since the air coming in from the surroundings is at the surrounding temperature. It is important that there is a natural flow of air through the system, so that the warm air from the exhaust does not go into the inlet. The system is indirect – there is a secondary loop which captures the sun's heat, and a heat exchanger which transfers heat between the two different fluids.
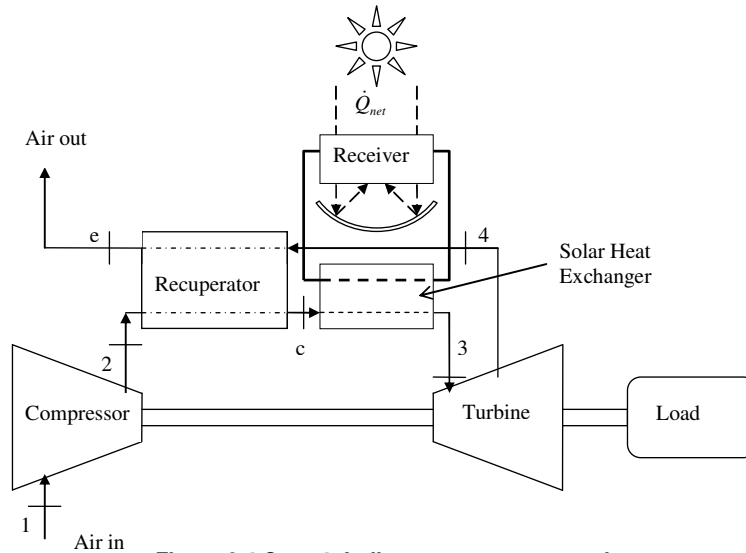

Figure 3.4 Case 4: Indirect system, open cycle.

3.3 Entropy generation in the solar thermal Brayton cycle components

Six different components were identified in the previous section. Not all of them are present in the open and direct solar thermal Brayton cycle. However, it is useful to show the entropy generation rate equations which can be used for each of these six components:

- Solar collector (receiver)
- Recuperator
- Solar heat exchanger (only in indirect systems)
- Radiator (only for closed cycles)
- Compressor
- Turbine

For each of these components, the entropy generation rate is derived using equations 2.12 – 2.14. These equations are then compared with the equations found from the literature in Appendix B.

3.3.1 Solar collector (receiver)

The entropy generation rate in the receiver is given in equation 3.1 for an ideal gas working fluid. Equations 2.13 and 2.14 are employed in the derivation of this equation. $\dot{Q}*$ is the rate of heat transfer from the apparent sun's temperature as an exergy source, $T*$. The rate of heat loss due to convection and radiation is shown in equation 3.2. Equation 3.1 is similar to equations 16, 17, 19 and 24 in the entropy generation table (Appendix B):

$$\dot{S}_{gen} = -\frac{\dot{Q}*}{T*} + \frac{\dot{Q}_0}{T_0} + \dot{m}c_{p0}\ln\left(\frac{T_e}{T_i}\right) - \dot{m}R\ln\left(\frac{P_e}{P_i}\right)$$

(3.1)

$$\dot{Q}_0 = \dot{Q}_{loss} = \dot{Q}_{rad} + \dot{Q}_{conv}$$

(3.2)

3.3.2 Recuperator

The entropy generation rate in the recuperator is shown in equation 3.3. Again, equations 2.13 and 2.14 are required for its derivation.

$$\dot{S}_{gen} = \dot{m}c_{p0}\ln\left[\frac{T_2 T_4}{T_1 T_3}\left(\frac{P_2 P_4}{P_1 P_3}\right)^{(1-k)/k}\right] + \frac{\dot{Q}_{loss,reg}}{T_0}$$

(3.3)

The fluid going from T_1 to T_2 is the hot stream and the fluid going from T_3 to T_4 is the cold stream in the heat exchanger as shown in Figure 2.28. This equation is similar to equations 16, 17, 19 and 28 found in the entropy generation table (Appendix B). According to Ordóñez and Bejan (2000) (equation 29 in Appendix B), entropy is also generated due to the discharge at the recuperator in an open cycle - hence equation 3.4. The equation to be used in an analysis depends on the definition of the boundaries of the control volumes of the recuperator and the system.

$$\dot{S}_{gen} = \dot{m}c_{p0}\left[\ln\left[\frac{T_2 T_4}{T_1 T_3}\left(\frac{P_2 P_4}{P_1 P_3}\right)^{(1-k)/k}\right] + \frac{T_2 - T_0}{T_0}\right] + \frac{\dot{Q}_{loss,reg}}{T_0}$$

(3.4)

3.3.3 Compressor and turbine

Equations 3.5 and 3.6 show the equations for the entropy generation rates for the compressor and turbine. Equations 2.13 and 2.14 were employed to derive these equations. These equations are formulated in terms of the pressures and temperatures, which could be described by the isentropic efficiencies. These equations compare with equation 27 in the entropy generation table (Appendix B).

$$\dot{S}_{gen,c} = \dot{m}c_{p0i-e} \ln(T_e/T_i) - \dot{m}R\ln(P_e/P_i) \tag{3.5}$$

$$\dot{S}_{gen,t} = \dot{m}c_{p0i-e} \ln(T_e/T_i) - \dot{m}R\ln(P_e/P_i) \tag{3.6}$$

3.3.4 Solar heat exchanger (for indirect systems)

The solar heat exchanger will not be used in this study but its entropy generation rate is shown in equation 3.7. This equation is identical to the equation for entropy generation rate in the recuperator (equation 3.3) with reference to Figure 2.28.

$$\dot{S}_{gen} = \dot{m}c_{p0} \ln\left[\frac{T_2 T_4}{T_1 T_3}\left(\frac{P_2 P_4}{P_1 P_3} \right)^{(1-k)/k} \right] + \frac{\dot{Q}_{loss}}{T_0} \tag{3.7}$$

3.3.5 Radiator (used in a closed system)

The radiator is not used in this study but its entropy generation is given for interest's sake. The entropy generation rate depends on the type of heat exchanger used for the radiator. Equation 3.8 is derived for the radiator if fins are used to cool down the working fluid (being an ideal gas) with a natural external flow (being air):

$$\dot{S}_{gen} = \frac{\dot{Q}_B}{T_B} + \dot{m}c_{p0} \ln\left(\frac{T_e}{T_i} \right) - \dot{m}R\ln\left(\frac{P_e}{P_i} \right) \tag{3.8}$$

where the subscript, B, refers to the base where the fins are attached (see Appendix B, equations 10 - 12). According to Bejan (1982), equation 3.8 can also be written as:

$$\dot{S}_{gen} = N\left[\frac{\dot{Q}_{B,sngl}(T_B - T_\infty)}{T_\infty^2} + \frac{F_D V_\infty}{T_\infty} \right] + \dot{m}c_{p0} \ln\left(\frac{T_e}{T_i} \right) - \dot{m}R\ln\left(\frac{P_e}{P_i} \right) \tag{3.9}$$

where it is assumed that $\dot{Q}_B = N\dot{Q}_{B,sngl}$ and N = number of fins.

3.4 Exergy analysis for the system

Consider Case 2 (Section 3.2.2). Taking a control volume around the system and assuming steady-state, it can be determined where exergy is crossing the boundary. This is shown in Figure 3.5.
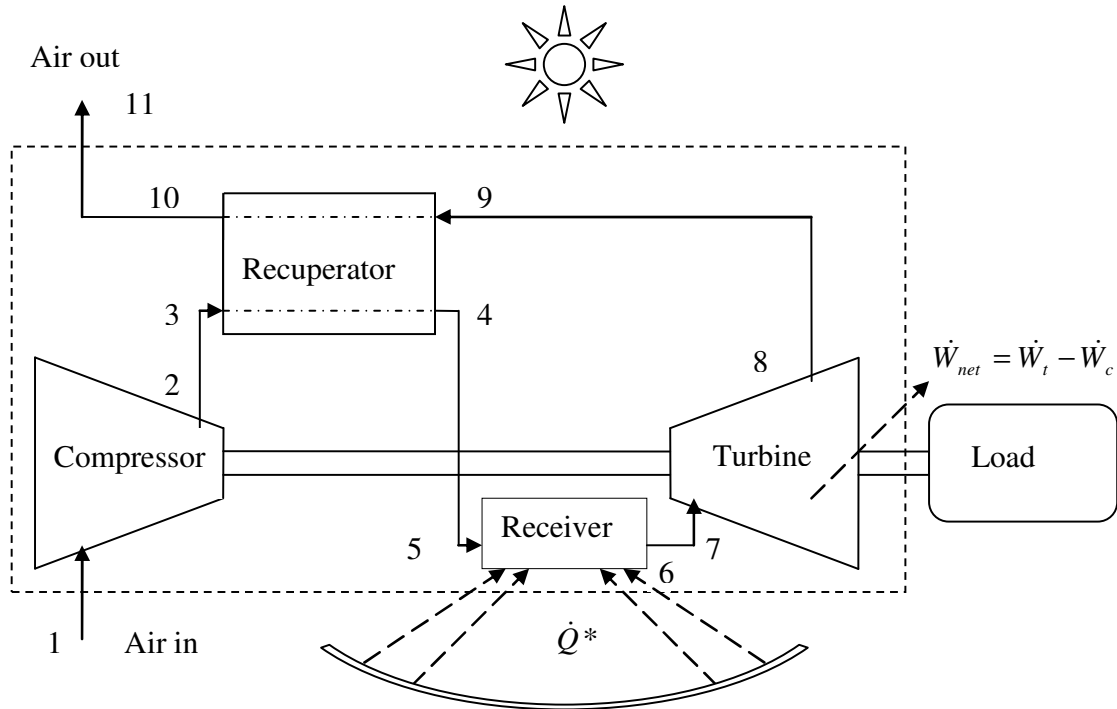

Figure 3.5 Control volume around the open and direct solar thermal Brayton cycle to perform an exergy analysis.

An exergy analysis is performed for the system and it is assumed that $V_1 = V_{11}$ and $z_1 = z_{11}$. Take note that the inlet and outlet temperatures of the system are not the same, but the pressures are. Also note that $T_{10} = T_{11}$ as it is assumed that the control volume boundary is very close to the hot stream exit of the recuperator. The following equation arises:

$$T_0\dot{S}_{gen} = \dot{m}e_i - \dot{m}e_e + \left(1 - \frac{T_0}{T*}\right)\dot{Q}* - \dot{W}_t + \dot{W}_c$$

$$\therefore T_0\dot{S}_{gen} = \dot{m}\left[h_i - h_e - T_0(s_i - s_e) + \frac{1}{2}(V_i^2 - V_e^2) + g(z_i - z_e)\right] + \left(1 - \frac{T_0}{T*}\right)\dot{Q}* - \dot{W}_{net}$$

(3.10)

or

$$\dot{W}_{net} = \dot{W}_t - \dot{W}_c = -T_0 \dot{S}_{gen} + \left(1 - \frac{T_0}{T*}\right)\dot{Q}* + \dot{m}c_{p0}(T_1 - T_{11}) - \dot{m}T_0 c_{p0} \ln\left(\frac{T_1}{T_{11}}\right)$$ (3.11)

Furthermore, the total internal entropy generation rate of the system can be written in terms of the sum of the entropy generation rate of each component and duct in the system. Thus, we have the total internal entropy generation rate from Section 3.3 as:

$$\dot{S}_{gen} =$$

$$\left[-\dot{m}c_{p0} \ln\left(\frac{T_1}{T_2}\right) + \dot{m}R \ln\left(\frac{P_1}{P_2}\right)\right]_{compressor} +$$

$$\left[\frac{\dot{Q}_{loss}}{T_0} + \dot{m}c_{p0} \ln\left(\frac{T_3}{T_2}\right) - \dot{m}R \ln\left(\frac{P_3}{P_2}\right)\right]_{duct\,23} +$$

$$\left[\dot{m}c_{p0} \ln\left[\frac{T_{10}T_4}{T_9 T_3}\left(\frac{P_{10}P_4}{P_9 P_3}\right)^{(1-k)/k}\right] + \frac{\dot{Q}_{loss}}{T_0}\right]_{recuperator} +$$

$$\left[\frac{\dot{Q}_{loss}}{T_0} + \dot{m}c_{p0} \ln\left(\frac{T_5}{T_4}\right) - \dot{m}R \ln\left(\frac{P_5}{P_4}\right)\right]_{duct\,45} +$$

$$\left[-\frac{\dot{Q}*}{T*} + \frac{\dot{Q}_0}{T_0} + \dot{m}c_{p0} \ln\left(\frac{T_6}{T_5}\right) - \dot{m}R \ln\left(\frac{P_6}{P_5}\right)\right]_{receiver} +$$

$$\left[\frac{\dot{Q}_{loss}}{T_0} + \dot{m}c_{p0} \ln\left(\frac{T_7}{T_6}\right) - \dot{m}R \ln\left(\frac{P_7}{P_6}\right)\right]_{duct\,67} +$$

$$\left[-\dot{m}c_{p0} \ln\left(\frac{T_7}{T_8}\right) + \dot{m}R \ln\left(\frac{P_7}{P_8}\right)\right]_{turbine} +$$

$$\left[\frac{\dot{Q}_{loss}}{T_0} + \dot{m}c_{p0} \ln\left(\frac{T_9}{T_8}\right) - \dot{m}R \ln\left(\frac{P_9}{P_8}\right)\right]_{duct\,89}$$ (3.12)

Equation 3.12 can then be substituted into equation 3.11 to get the net power output for the open and direct solar thermal Brayton cycle. The net power output is then written in terms of the total entropy generation rate of each of the components and ducts in the system. This equation for the

net power output is the objective function, which should be maximised by optimising the geometry that describes the temperatures and pressures at each point in the system.

3.5 Description of the physical model

An equation is now available describing the net power output of the open and direct solar thermal Brayton cycle in terms of temperatures, pressures, mass flow rate and other constants. The physical models used to describe the geometry of the solar receiver and recuperator will now be shown. Variables also exist, which can be treated as parameters. The objective function can then be formulated in terms of geometry variables and system parameters.

3.5.1 Geometry variables

3.5.1.1 Geometry of the receiver

From the literature, it is concluded that a cavity receiver should be used when an efficient solar thermal Brayton cycle is required. Shuai et al. (2008), Prakash et al. (2009) and Sendhil Kumar and Reddy (2008) investigated the optimisation and performance of different cavity receivers. Sendhil Kumar and Reddy (2007) compared different types of cavity receivers numerically and found that the modified cavity receiver, as shown in Figures 2.25 and 2.26, experiences lower convection heat losses than those of the other receivers and suggested that it may be preferred in a solar dish collector system. In the numerical modelling, A_w is the inner-heat transfer area, which includes the inner-curved and bottom plane areas. Its size depends on the bottom aperture opening area, A_a. The size of the aperture opening is determined by the flux distribution (focal image characteristics of the fuzzy focal solar dish). The receiver inner surface is made up of closely wound copper tubing – these tubes are placed very closely to touch each other to form a continuous hemispherical surface. The convection heat loss takes place through the receiver aperture. It is suggested that an area ratio of A_w/A_a = 8 is used when minimum heat loss is required (Reddy and Sendhil Kumar, 2009).

Reddy and Sendhil Kumar (2008) investigated the modified cavity further by including the contribution of radiation losses and found that, for A_w/A_a = 8 and a 0° tilt angle (vertical aperture plane), the ratio of the contribution of radiation to convection loss is 47:52. This ratio shifts to 57:43 when the tilt angle is 90°. This means that the ratio of radiation heat loss to convection heat loss is a function of receiver inclination and varies between approximately 0.9 and 1.33. From this data, it is assumed that $\dot{Q}_{loss-rad} \approx \dot{Q}_{loss-conv}$ or $\dot{Q}_0 \approx 2\dot{Q}_{loss-conv}$ for this modified cavity receiver. From Reddy and Sendhil Kumar (2009), for A_w/A_a = 8 at a vertical

position (cavity aperture in vertical plane), $Nu = 27$. This number becomes almost half the value when the cavity receiver is in the horizontal plane. The most heat loss would thus take place when the cavity receiver is placed vertically (when the sun is on the horizon and the collector faces the sun). This would seldom be the case. An average of $Nu = 20$ would be more accurate since the cavity receiver would be between 0° and 90° most of the time. The most accurate Nusselt number would be the one given by Reddy and Sendhil Kumar (2009), for their three-dimensional model in terms of receiver inclination, and will be used for this analysis:

$$Nu_D = 0.698 Gr_D^{0.209} \left(1 + \cos \beta\right)^{0.968} \left(T_w / T_\infty\right)^{-0.317} \left(d / D\right)^{0.425} \tag{3.13}$$

The convection heat transfer coefficient can be calculated with

$$h_{conv} = \frac{Nu_D k}{D} \tag{3.14}$$

The rate of heat loss from the modified cavity receiver due to convection and radiation can be approximated with

$$\dot{Q}_0 = 1.396 Gr_D^{0.209} \left(1 + \cos \beta\right)^{0.968} \left(T_w / T_\infty\right)^{-0.317} \left(d / D\right)^{0.425} \left(k A_a / D\right)\left(T_w - T_\infty\right) \tag{3.15}$$

According to Reddy and Sendhil Kumar (2009), the minimum heat loss occurs when $A_w / A_a = 8$. From equation 2.3, the modified cavity receiver diameter for minimum heat loss can be calculated with:

$$D = 2 \sqrt{\left(\frac{A_w + A_a}{3\pi}\right)} \tag{3.16}$$

Equation 3.17 gives the modified cavity receiver diameter as a function of the receiver aperture, d, for minimum heat loss:

$$D = 2 \sqrt{\left(\frac{9 A_a}{3\pi}\right)} = 2 \sqrt{\left(\frac{3 d^2}{4}\right)} = \sqrt{3} d \tag{3.17}$$
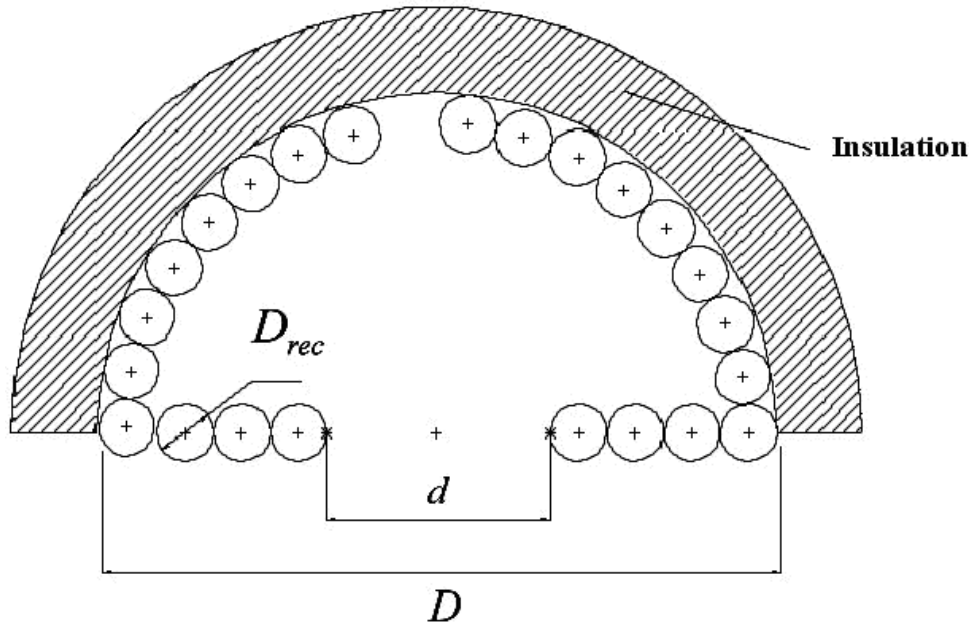
Figure 3.6 Geometry of the cavity receiver constructed with a circular tube.
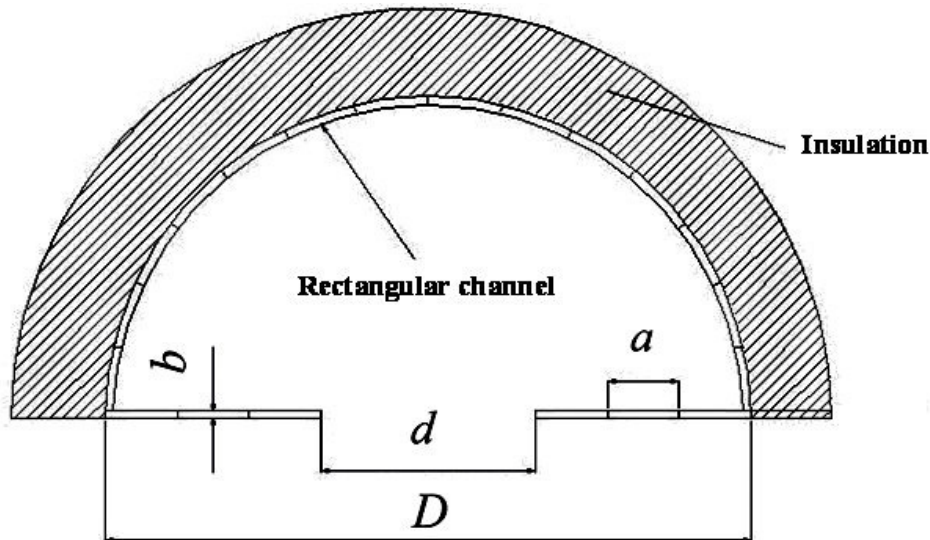

Figure 3.7 Cavity constructed with the use of a rectangular channel (plate) and its dimensions.

The receiver inner surface is made up of closely wound copper tubing with diameter, D_{rec} – these tubes are placed very closely to touch each other to form a continuous hemispherical surface. The working fluid is pumped concentrically through the tube, as is shown in Figure 3.6. The tube with diameter, D_{rec}, and length, L_{rec}, constructs the cavity receiver and its aperture. Another method would be to use flat plate to construct a rectangular channel (Figure 3.7). The receiver channel with hydraulic diameter, $D_{h,rec}$, length, L_{rec}, and aspect ratio, a/b_{rec}, constructs

the cavity receiver and its aperture. Both of these models will be used in the analysis and the results will be compared.

Using the definition of hydraulic diameter for a rectangular channel (the hydraulic diameter is four times the cross-sectional area divided by the wetted perimeter), the longer side, a, can be described with

$$a = \frac{D_{h,rec}\left(\left(\dfrac{a}{b}\right)_{rec} + 1\right)}{2} \tag{3.18}$$

since

$$D_{h,rec} = \frac{4a}{2\left(\left(\dfrac{a}{b}\right)_{rec} + 1\right)} \tag{3.19}$$

Also, the aperture diameter is derived as:

$$d = \sqrt{\frac{D_{h,rec}L_{rec}\left(\left(\dfrac{a}{b}\right)_{rec} + 1\right)}{4\pi}} \tag{3.20}$$

since

$$A_w = aL_{rec} \tag{3.21}$$

When the receiver walls are constructed by winding a circular tube, the aperture diameter, d, can be calculated using $a/b_{rec} = 1$, in equation 3.20.

3.5.1.2 Geometry of the recuperator

On recommendation of Shah (2005), the counterflow plate-type heat exchanger is considered for the recuperator. In this work, only one recuperator is considered for the system, even though it might seem that the splitting up of the mass flow rate into separate heat exchangers is more

63

attractive. It was decided to rather keep it simple and also avoid the extra cost and piping due to an extra heat exchanger(s).

The design and assembly will be as illustrated in Figure 3.8. This means that the mass flow rate is divided. Also $A_s = A_i = A_o$ and $A_s = 2aL_{reg}$ (where a is the long side of the rectangle forming the channel). The recuperator is formed by stacking plates and creating counterflow channels. Also note that in Figure 3.8, only a few plates are stacked to show the effect. The number of flow channels, n, in the recuperator depends on the recuperator height, H, channel height, b, and thickness of the channel-separating surface, t. This is shown in equation 3.22.

$$n = H/(t+b) = \frac{H}{t + D_{h,reg}\left((a/b)_{reg}+1\right)/\left(2(a/b)_{reg}\right)} \qquad (3.22)$$
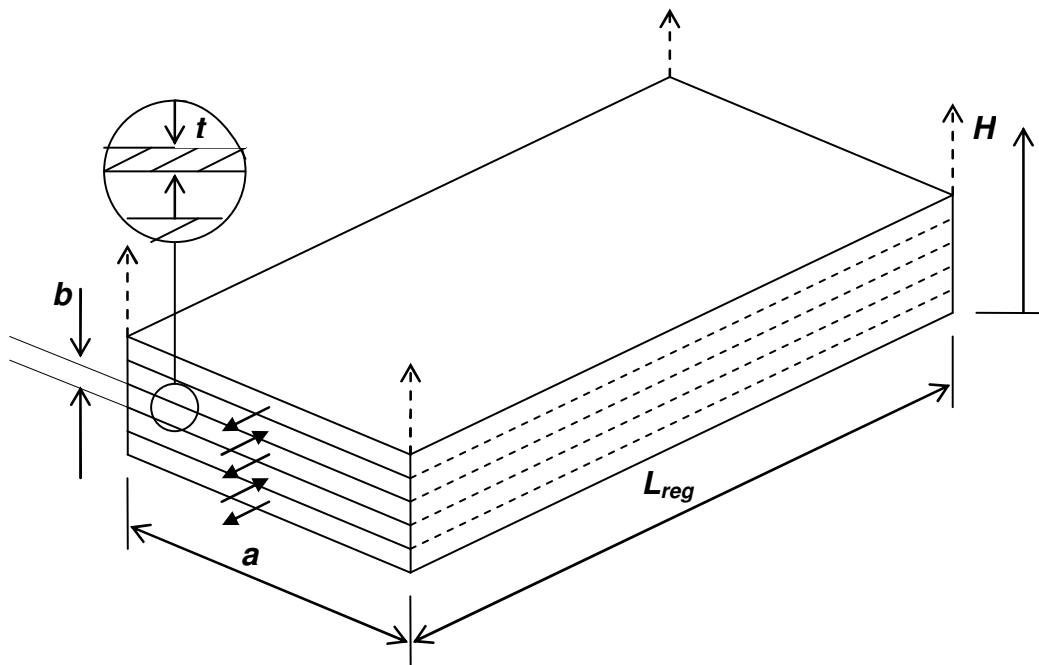

Figure 3.8 Counterflow plate-type recuperator.

The mass flow rate per channel is calculated with:

$$\dot{m}_{reg} = \frac{2\dot{m}}{n} \qquad (3.23)$$

The surface area, A_s, for a channel is given by:

$$A_s = 2(a+b)L_{reg} = D_{h,reg} L_{reg} \left(\frac{a}{b}_{reg} + 1 \right) \left(1 + \left(\frac{a}{b} \right)_{reg}^{-1} \right) \tag{3.24}$$

and the Reynolds number for a rectangular channel is:

$$\mathrm{Re} = \frac{4\dot{m}_{reg} \left(\dfrac{a}{b} \right)_{reg}}{\mu D_{h,reg} \left(\dfrac{a}{b}_{reg} + 1 \right)^2} \tag{3.25}$$

The average velocity is calculated as:

$$V_{avg} = \frac{4\dot{m}_{reg} \left(\dfrac{a}{b} \right)_{reg}}{\rho D_{h,reg}^{\ 2} \left(\dfrac{a}{b}_{reg} + 1 \right)^2} \tag{3.26}$$

The recuperator efficiency can be calculated using the $\varepsilon - NTU$ (effectiveness – number of transfer units) method, as suggested from the literature. The Gnielinski equation (Gnielinski, 1976) can be used to calculate the Nusselt number since small Reynolds numbers are most likely to be present in a single channel of the recuperator. The first Petukhov equation (Petukhov, 1970) is used to calculate the friction factor:

$$f = 0.79 \ln(\mathrm{Re}) - 1.64)^{-2} \tag{3.27}$$

Using the Gnielinski and Petukhov equations with the Reynolds number above gives:

$$Nu_D = \frac{\Pr(\mathrm{Re} - 1000) f / 8}{1 + 12.7 (f/8) \left(\Pr^{2/3} - 1 \right)} \tag{3.28}$$

with

$$h = \frac{k Nu_D}{D_{h,rec}} \tag{3.29}$$

With equation 3.29, the convection heat transfer coefficients for the hot and cold stream (h_c and h_h) can be calculated. When these are available, the overall heat transfer coefficient is calculated:

$$U = \left(\frac{1}{h_c} + 2R_f + \frac{L_{reg}}{k_{solid}} + \frac{1}{h_h} \right)^{-1} \tag{3.30}$$

where the fouling factor R_f = 0.004 for air, according to Çengel (2006). The number of transfer units (NTU) is calculated:

$$NTU = \frac{UA_s}{\dot{m}_{reg} c_p} \tag{3.31}$$

and

$$c = \frac{c_{p,c}}{c_{p,h}} \tag{3.32}$$

The recuperator effectiveness can be calculated with equation 3.33.

$$\varepsilon = \frac{1 - \exp\left[-NTU(1-c) \right]}{1 - c \exp\left[-NTU(1-c) \right]} \tag{3.33}$$

According to Stine and Harrigan (1985), Weston (2000) and Çengel (2006), the heat exchanger efficiency and heat exchanger effectiveness are defined the same way for the recuperator in this analysis (with reference to Figure 3.5):

$$\eta_{reg} = \varepsilon = \frac{\dot{Q}}{\dot{Q}_{max}} = \frac{\dot{m} c_p (T_4 - T_3)}{\dot{m} c_p (T_9 - T_3)} = \frac{T_4 - T_3}{T_9 - T_3} \tag{3.34}$$

This efficiency will help to produce the temperatures and pressures necessary to describe the objective function. The importance of the recuperator efficiency is shown in Chapter 2.

With the use of the definitions of the Reynolds number (equation 3.25) and the friction factor (equation 3.27) and the definition of the pressure drop (Çengel, 2006), the pressure drop through the recuperator is derived in terms of the geometry variables as:

$$\Delta P = \left(0.79 \ln \frac{4\dot{m}_{reg} (a/b)_{reg}}{\mu D_{h,reg} (a/b_{reg} +1)^2} - 1.64 \right)^{-2} \left(\frac{8\dot{m}_{reg}^2 (a/b)_{reg}^2}{\rho (a/b_{reg} +1)^4} \right) \left(\frac{L_{reg}}{D_{h,reg}^5} \right)$$ (3.35)

3.5.2 Parameters

According to Snyman (2009), the pressure ratio, r, of the compressor should be chosen to be a parameter. The objective function can be maximised and the optimum geometry can be found for each pressure ratio in the compressor's range. When considering the mass flow rate through the system, it depends on the compressor, which, in turn, depends on the turbine. There are, unfortunately, many different compressor and turbine designs available. The task and cost of designing one's own turbine and compressor configuration for a specific system, by shaping its geometry using the method of entropy generation minimisation, is in itself a mammoth task and can be considered or recommended for further study. In this work, however, the compressor and turbine configuration comes from an existing source chosen for its low cost, availability and reliability.

From the literature, the advantages of using the micro-turbines from the Garrett range are evident and they will be used in the analysis. The Garrett micro-turbines (Appendix D) as well as their turbine and compressor maps (Garrett, 2009) are freely available in South Africa. For the compressor of a specific micro-turbine, the compressor efficiency, mass flow rate and pressure ratio are intrinsically coupled to each other. Garrett (2009) also gives the turbine efficiencies for each of its micro-turbines. Thanks to these existing micro-turbines from Garrett, the compressor pressure ratio as a parameter would fix the mass flow rate and compressor efficiency as parameters as well. Figure 3.9 shows the compressor map of a micro-turbine (GT2259) with micro-turbine model number 9 (*MT* = 9 in Appendix D). In the compressor map, the coupling of compressor efficiency, mass flow rate and pressure ratio are shown. The rotational speed in revolutions per minute is also shown. Note that the highest compressor efficiency is on the island in the middle of the compressor map (between two mass flow rate values: $\dot{m}_{low}$ and $\dot{m}_{high}$ and between two pressure ratio values: r_{low} and r_{high}). These pressure ratio and mass flow rate ranges are shown for each micro-turbine in Appendix D. When only considering the highest compressor efficiency for the analysis, the pressure ratio (r) – mass flow rate ($\dot{m}$) relation can

be described with a straight line. Hence the equation to find the mass flow rate when the pressure ratio is fixed:

$$\dot{m} = \frac{\left(\dot{m}_{high} - \dot{m}_{low}\right)}{\left(r_{high} - r_{low}\right)}\left(r - r_{low}\right) + \dot{m}_{low} \qquad (3.36)$$

An optimum pressure ratio (or operating condition) should exist for a specific micro-turbine, which would (with its optimised geometry) give the maximum net power output.
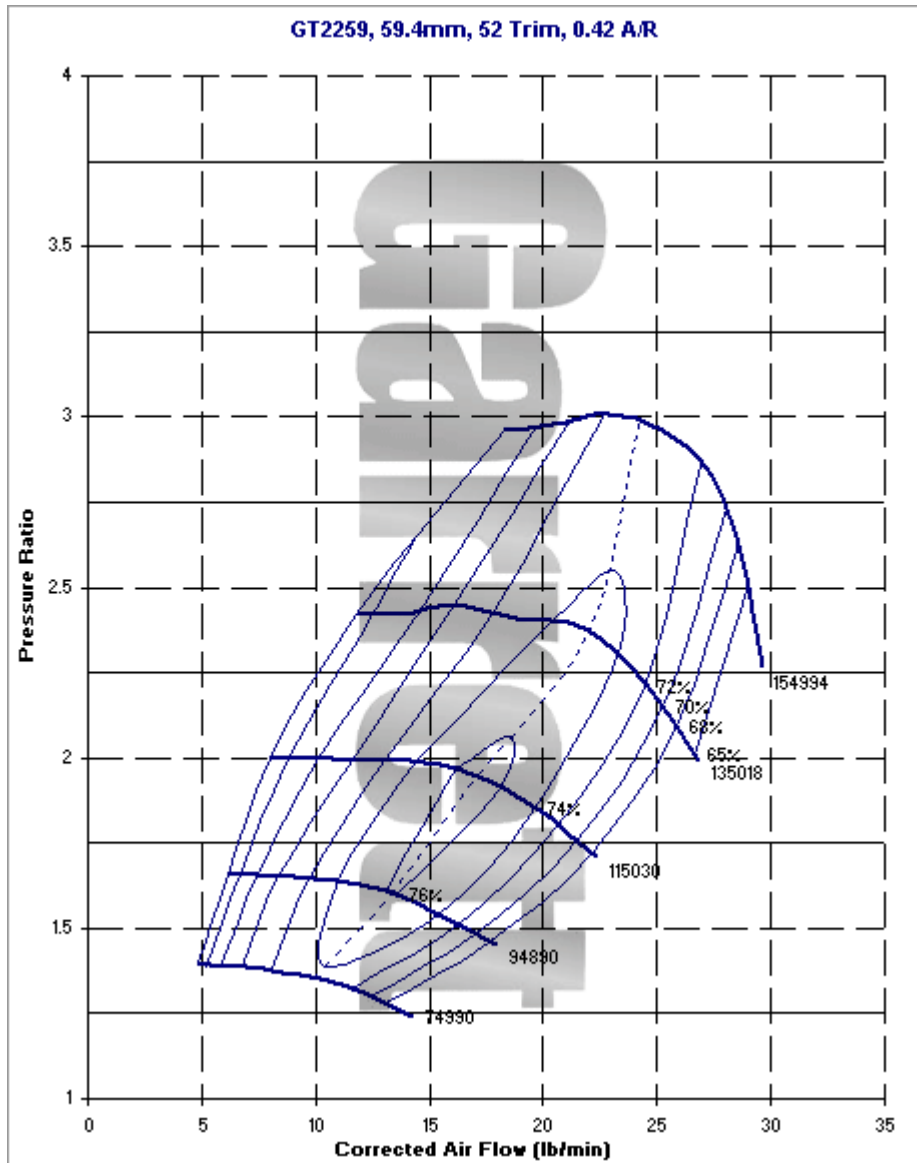

Figure 3.9 Compressor map for a micro-turbine from Garrett (Garrett, 2009).

3.6 Temperatures and pressures in terms of geometry variables

For the objective function, the temperatures and pressures at each point in the system (Figure 3.5) can be determined in terms of the geometry variables. The six geometry variables are:

$D_{h,rec}$ - Hydraulic diameter of the cavity receiver channel (or tube diameter, D_{rec})

L_{rec} - Tube or channel length of the cavity receiver

a/b_{rec} - Aspect ratio of the receiver channel (negligible when the receiver walls are made from circular tube)

$D_{h,reg}$ - Hydraulic diameter of the recuperator channels

L_{reg} - Length of the recuperator channels

a/b_{reg} - Aspect ratio of the recuperator channels

The temperatures and pressures at each point in the system (Figure 3.5) can be determined as is explained below. The process of finding the pressures and temperatures can be divided into five phases. Each phase has a number of steps.

Phase 1 (Pre-receiver):
The inlet temperature of the system is:

$$T_1 = 300 \text{ K} \tag{3.37}$$

T_2 is calculated using the compressor isentropic efficiency, η_c, and the compressor pressure ratio, r, as parameters. T_3 can then be calculated:

$$T_2 = T_1 \left[1 + (K-1)/\eta_c \right] \tag{3.38}$$

where

$$K = r^{k-1/k} \tag{3.39}$$

$$T_3 = T_2 - \Delta T_{23} \tag{3.40}$$

A constant is assumed for ΔT_{23} and also for all the other temperature drops in the ducting between components. It is important to note that the temperature in the ducting between components actually depends on the size of the duct and that the size of the ducting might also play a role in the shadow effect of the collector.

Phase 2 (Receiver):

Guess T_5 = 800 K, and then calculate T_6 with:

$$T_6 = \frac{\dot{Q}_{net}}{\dot{m}c_p} + T_5 \tag{3.41}$$

The net rate of absorbed heat in the cavity receiver, $\dot{Q}_{net}$, is a function of the receiver aperture diameter, d. This function can be determined with the use of a sizing algorithm. In this analysis, the sizing algorithm by Stine and Harrigan (1985) is used, as explained in Appendix A. The function determined by the sizing algorithm can be approximated with the discrete least-squares approximation method (Burden and Faires, 2005) ($\dot{Q}_{net} = \sum_{i=0}^{10} x_i d^i$). $\dot{Q}_{net}$ can be written in terms of $D_{h,rec}$, L_{rec} and a/b_{rec} (the geometric variables for the cavity receiver) since $A_w = 8A_a = 8\pi d^2/4 = a_{rec}L_{rec}$. In equation 3.20, d is written in terms of the receiver geometry variables. The net absorbed heat rate can be written in terms of the receiver geometry variables:

$$\dot{Q}_{net} = \sum_{i=0}^{10} x_i \left(\sqrt{\frac{D_{h,rec} L_{rec} \left((a/b)_{rec} + 1 \right)}{4\pi}} \right)^i \tag{3.42}$$

Note that when a circular tube constructs the cavity receiver, a/b_{rec} = 1. With the use of equation 3.42, T_6 can be written in terms of the geometry variables (equation 3.43). For a receiver constructed with circular tube, equation 3.43 can be used with a/b_{rec} = 1. T_7 is calculated with an assumed value for ΔT_{67}.

$$T_6 = \frac{\sum_{i=0}^{10} x_i \left(\sqrt{\dfrac{D_{h,rec} L_{rec} \left((a/b)_{rec} + 1 \right)}{4\pi}} \right)^i}{\dot{m} c_p} + T_5 \tag{3.43}$$

$$T_7 = T_6 - \Delta T_{67} \tag{3.44}$$

Phase 3 (Pressure field):

The inlet pressure of the system, P_1 and the exit pressure of the compressor, P_2 can be calculated using the following equations:

$$P_1 = P_{atm} \tag{3.45}$$

$$P_2 = rP_1 \tag{3.46}$$

$$P_3 = P_2 (1 - \Delta P_{23}) \tag{3.47}$$

P_3, P_5, P_7 and P_8 are calculated with an assumed pressure drop in the ducts. P_4 and P_9 can be calculated with equations 3.48 and 3.53 respectively. These equations are written in terms of the geometry variables of the recuperator and are derived using equation 3.35.

$$P_4 = P_3 - \left(0.79 \ln \frac{4 \dot{m}_{reg} (a/b)_{reg}}{\mu D_{h,reg} (a/b_{reg} + 1)^2} - 1.64 \right)^{-2} \left(\frac{8 \dot{m}_{reg}{}^2 (a/b)_{reg}{}^2}{\rho (a/b_{reg} + 1)^4} \right) \left(\frac{L_{reg}}{D_{h,reg}{}^5} \right) \tag{3.48}$$

$$P_5 = P_4 (1 - \Delta P_{45}) \tag{3.49}$$

P_6 is calculated with equation 3.50, which is written in terms of the receiver geometry variables and derived using equation 3.35. Equation 3.50a is for a receiver constructed with a rectangular channel (plate) and equation 3.50b is for a receiver constructed with a circular tube.

Plate:

$$P_6 = P_5 - \left(0.79\ln\frac{4\dot{m}(a/b)_{rec}}{\mu D_{h,rec}\left((a/b)_{rec}+1\right)^2} - 1.64\right)^{-2}\left(\frac{8\dot{m}^2(a/b)_{rec}^{\;2}}{\rho\left((a/b)_{rec}+1\right)^4}\right)\left(\frac{L_{rec}}{D_{h,rec}^{\;5}}\right) \qquad (3.50a)$$

Tube:

$$P_6 = P_5 - \left(0.79\ln\frac{4\dot{m}}{\mu\pi D_{h,rec}} - 1.64\right)^{-2}\left(\frac{8\dot{m}^2}{\rho\pi^2}\right)\left(\frac{L_{rec}}{D_{h,rec}^{\;5}}\right) \qquad (3.50b)$$

$$P_7 = P_6\left(1 - \Delta P_{67}\right) \qquad (3.51)$$

The system exit pressure, P_{11}, is the same as the system inlet pressure, P_1, as shown in equation 3.52. Also note that P_{10} = P_{11}. P_9 can be calculated using the system exit pressure:

$$P_{11} = P_1 \qquad (3.52)$$

$$P_9 = P_{10} + \left(0.79\ln\frac{4\dot{m}_{reg}(a/b)_{reg}}{\mu D_{h,reg}\left(a/b_{reg}+1\right)^2} - 1.64\right)^{-2}\left(\frac{8\dot{m}_{reg}^{\;2}(a/b)_{reg}^{\;2}}{\rho\left(a/b_{reg}+1\right)^4}\right)\left(\frac{L_{reg}}{D_{h,reg}^{\;5}}\right) \qquad (3.53)$$

$$P_8 = P_9\left(1 + \Delta P_{89}\right) \qquad (3.54)$$

Phase 4 (Post-turbine):

T_8 is calculated with equation 3.55 with the use of the turbine isentropic efficiency, η_t, and the turbine pressure ratio. T_{10} is calculated with the recuperator efficiency, η_{reg} (equation 3.33). Also note that T_{11} = T_{10}.

$$T_8 = T_7\left[1 - \eta_t\left[1 - \frac{1}{\left(P_7/P_8\right)^{((k-1)/k)}}\right]\right] \qquad (3.55)$$

$$T_9 = T_8 - \Delta T_{89} \qquad (3.56)$$

$$T_{10} = T_9 - \eta_{reg}\left(T_9 - T_2\right) \tag{3.57}$$

Phase 5 (Iteration):

T_4 is calculated with the recuperator efficiency. T_5 can then be calculated and is used as the new approximation for T_5 in Phase 1. The iteration continues until the error is smaller than 1×10^{-3}. When the iteration is done, the temperatures and pressures are established and can be used in the objective function.

$$T_4 = T_3 + \eta_{reg}\left(T_9 - T_3\right) \tag{3.58}$$

$$T_5 = T_4 - \Delta T_{45} \tag{3.59}$$

3.7 The objective function

The objective function (equations 3.11 and 3.12) can be written in terms of geometry variables, parameters and constants. When looking at the previous section, it should be clear that the objective function, in terms of all the variables, parameters and constants, is very complex and is not shown. Note, however, the cancelling out of the following terms (from equation 3.12 in equation 3.11) so that:

$$\frac{\dot{Q}*T_0}{T*} - \dot{Q}_0 + \dot{Q}* - \frac{\dot{Q}*T_0}{T*} = \dot{Q}_{net} \tag{3.60}$$

The final objective function can be written as:

$$\dot{W}_{net} = \dot{Q}_{net} + \dot{m}c_{p0}(T_1 - T_{11}) - \dot{m}T_0 c_{p0} \ln\left(\frac{T_1}{T_{11}}\right)$$

$$-T_0\left[-\dot{m}c_{p0}\ln\left(\frac{T_1}{T_2}\right) + \dot{m}R\ln\left(\frac{P_1}{P_2}\right)\right]_{compressor}$$

$$-T_0\left[\frac{\dot{Q}_{loss}}{T_0} + \dot{m}c_{p0}\ln\left(\frac{T_3}{T_2}\right) - \dot{m}R\ln\left(\frac{P_3}{P_2}\right)\right]_{duct\,23}$$

$$-T_0\left[\dot{m}c_{p0}\ln\left[\frac{T_{10}T_4}{T_9 T_3}\left(\frac{P_{10}P_4}{P_9 P_3}\right)^{(1-k)/k}\right] + \frac{\dot{Q}_{loss}}{T_0}\right]_{recuperator}$$

$$-T_0\left[\frac{\dot{Q}_{loss}}{T_0} + \dot{m}c_{p0}\ln\left(\frac{T_5}{T_4}\right) - \dot{m}R\ln\left(\frac{P_5}{P_4}\right)\right]_{duct\,45}$$

$$-T_0\left[\dot{m}c_{p0}\ln\left(\frac{T_6}{T_5}\right) - \dot{m}R\ln\left(\frac{P_6}{P_5}\right)\right]_{receiver}$$

$$-T_0\left[\frac{\dot{Q}_{loss}}{T_0} + \dot{m}c_{p0}\ln\left(\frac{T_7}{T_6}\right) - \dot{m}R\ln\left(\frac{P_7}{P_6}\right)\right]_{duct\,67}$$

$$-T_0\left[-\dot{m}c_{p0}\ln\left(\frac{T_7}{T_8}\right) + \dot{m}R\ln\left(\frac{P_7}{P_8}\right)\right]_{turbine}$$

$$-T_0\left[\frac{\dot{Q}_{loss}}{T_0} + \dot{m}c_{p0}\ln\left(\frac{T_9}{T_8}\right) - \dot{m}R\ln\left(\frac{P_9}{P_8}\right)\right]_{duct\,89} \tag{3.61}$$

Keep in mind that each temperature and pressure in equation 3.61 is defined in terms of parameters and geometry variables, as shown in Section 3.6.

3.8 Constraints

Constraint 1:

The maximum cavity receiver aperture diameter is constrained. The minimum concentration ratio, CR_{min}, will determine the maximum size of the cavity aperture relative to the concentrator area.

From the literature, the concentration ratio seems to be more than 100 for receiver temperatures of more than 1 000 K (see Section 2.3.2). For this work, $CR \geq 100$, hence we have:

$$\frac{\pi}{4}d^2 < A_{s,conc}/100$$

$$\frac{\pi}{4}\left(\frac{D_{h,rec}L_{rec}\left(\left(a/b\right)_{rec}+1\right)}{4\pi}\right) < A_{s,conc}/100 \tag{3.62}$$

$$\frac{D_{h,rec}L_{rec}\left(\left(a/b\right)_{rec}+1\right)}{16} - \frac{A_{s,conc}}{100} < 0$$

The constraint above is for a receiver constructed with a rectangular channel. For a receiver constructed with a circular tube, the same constraint can be used, but with $\left(a/b\right)_{rec}=1$

Constraint 2:

The receiver aperture diameter, d, has a minimum constraint to keep the aperture size from going too small or negative. $Wn(2)$ is the second term in the vector Wn (used in the function 'collector' – see Appendix C).

$$Wn(2) < \sqrt{\frac{D_{h,rec}L_{rec}\left(\left(a/b\right)_{rec}+1\right)}{4\pi}}$$

$$Wn(2) - \sqrt{\frac{D_{h,rec}L_{rec}\left(\left(a/b\right)_{rec}+1\right)}{4\pi}} < 0 \tag{3.63}$$

Similarly, for a receiver constructed with circular tube, $\left(a/b\right)_{rec}=1$

Constraint 3:

The width of the rectangular channel, a, in the receiver cannot be larger than the distance between the aperture and the edge of the receiver. With the use of equation 3.17 from Section 3.5.1.1, this distance can be described with equation 3.64.

$$D = \sqrt{3}d \tag{3.17}$$

$$\left(\frac{\sqrt{3}-1}{2}\right)d \geq a \tag{3.64}$$

With equation 3.18 from Section 3.5.1.1, this constraint is written in terms of the geometry variables using equation 3.65.

$$a = \frac{D_{h,rec}\left(\left(a/b\right)_{rec}+1\right)}{2} \tag{3.18}$$

$$\frac{D_{h,rec}\left(\left(a/b\right)_{rec}+1\right)}{2} - \left(\frac{\sqrt{3}-1}{2}\right)\sqrt{\frac{D_{h,rec}L_{rec}\left(\left(a/b\right)_{rec}+1\right)}{4\pi}} \leq 0 \tag{3.65}$$

When a receiver constructed with a circular tube is used, at least two tube diameters should fit in the distance between the aperture edge and the edge of the receiver. Otherwise, the receiver would lose its cavity shape. This is shown in equation 3.66.

$$2D_{h,rec} - \left(\frac{\sqrt{3}-1}{2}\right)\sqrt{\frac{D_{h,rec}L_{rec}}{2\pi}} \leq 0 \tag{3.66}$$

Constraint 4:

The surface temperature of the receiver (of copper) should stay well below its melting temperature and below the maximum inlet temperature of the micro-turbines (more or less 1 220 K or 1 320 K intermittently according to Garrett (2009) and Shah (2005) - see Section 2.3.5 and Section 2.2.2.3.1). A maximum temperature of 1 200 K is chosen. The surface area of the rectangular receiver channel can be defined as:

$$A_s = D_{h,rec}L_{rec}\left(\left(a/b\right)_{rec}+1\right)\left(1+\left(a/b\right)_{rec}^{-1}\right) \tag{3.67}$$

Since turbulent flow is expected in the receiver tube or channel, the Nusselt number is defined as (Dittus and Boelter, 1930):

$$Nu = 0.023\,\mathrm{Re}_D^{0.8}\,\mathrm{Pr}^{0.4} \tag{3.68}$$

For a receiver constructed with a rectangular channel (plate), the maximum surface temperature can be defined as:

Plate :

$$T_{s,\max} = T_6 + \frac{\sum_{i=0}^{10} x_i \left(\sqrt{\frac{D_{h,rec} L_{rec} \left((a/b)_{rec} + 1 \right)}{4\pi}} \right)^i}{0.023 L_{rec} \left((a/b)_{rec} + 1 \right) \left(1 + (a/b)_{rec}^{-1} \right) k \, \mathrm{Pr}^{0.4} \left(\frac{4\dot{m}(a/b)_{rec}}{\mu D_{h,rec} \left((a/b)_{rec} + 1 \right)^2} \right)^{0.8}} \tag{3.69}$$

Note that equation 3.42 is used in the construction of equation 3.69, since $\dot{Q}_{net}$ is required to calculate the maximum surface temperature. When the receiver is constructed with the use of a circular tube, the maximum surface temperature can be defined as:

Tube :

$$T_{s,\max} = T_6 + \frac{\sum_{i=0}^{10} x_i \left(\sqrt{\frac{D_{rec} L_{rec}}{2\pi}} \right)^i}{0.023 \pi L_{rec} k \, \mathrm{Pr}^{0.4} \left(4\dot{m} / (\mu \pi D_{rec}) \right)^{0.8}} \tag{3.70}$$

Constraints 5 and 6:

The hydraulic diameter and length of the receiver is always positive:

$$-D_{h,rec} \leq 0 \tag{3.71}$$

$$-L_{rec} \leq 0 \tag{3.72}$$

Constraint 7:

The longer the recuperator, the more beneficial it is to the system from a heat transfer point. However, there needs to be a constraint on its length to make sure the system stays compact. The recuperator's length should not exceed the length of the radius of the dish concentrator. Since there is already a large concentrator, there is no sense in keeping the recuperator many times smaller than the dish to save space. A recuperator can perhaps fit underneath the space occupied by the dish concentrator with relative ease. Therefore:

$$L_{reg} \leq \sqrt{\frac{A_{s,conc}}{\pi}} = D/2 \tag{3.73}$$

Constraint 8:

This constraint is only necessary when the receiver walls are constructed using a rectangular channel. The channel should have an aspect ratio equal to or larger than 2.5 to ensure that the shape of the cavity receiver is maintained. Hence:

$$2.5 - \left(\frac{a}{b}\right)_{rec} \leq 0 \tag{3.74}$$

3.9 Constants / assumptions

The objective function relies on a number of constants. These constants would depend on the location and available space for the solar thermal power system and are therefore very location- and situation-specific. The most important constants are shown below. For each specific location and situation, a different optimum receiver and recuperator geometry would exist.

Environmental conditions:

- ➢ T_0 Surrounding average temperature (K)
- ➢ I Irradiance (W/m^2)
- ➢ w Non-dimensionalised wind factor (1 – 10) multiplied with convection heat transfer coefficient
- ➢ P_{atm} Atmospheric pressure (Pa)

Available space at location:

- ➢ $A_{s,conc}$ Parabolic dish concentrator area (m^2)
- ➢ H Available space for height of recuperator (m)
- ➢ L Available space for length of recuperator (m)

Concentrator and receiver:

- ➢ e_p Concentrator error
- ➢ φ_{rim} Rim angle of parabolic dish concentrator
- ➢ $refl$ Specular reflectivity of the concentrator
- ➢ $T_{s,max}$ Maximum allowable surface temperature of receiver
- ➢ β Inclination of receiver (90° for receiver aperture facing down)
- ➢ CR_{min} Minimum concentration ratio

Recuperator:

> t Heat exchanger wall thickness between hot and cold streams
> k Recuperator material conductivity

3.10 Summary

In this chapter, the objective function to be optimised was formulated and the physical model to be analysed was described. The different possibilities of arrangements of components in the solar thermal Brayton cycle were identified and the uniqueness of the open and direct solar thermal Brayton cycle was shown. The rate of entropy generation in each of the system's components was identified. The total rate of entropy generation was obtained for the system by adding the entropy generation rates of each system component. The net power output of the system was linked with the total entropy generation rate by doing an exergy analysis for the whole system. The construction of the objective function in terms of the geometry variables of the receiver and recuperator was shown. The recuperator and receiver models were described in terms of the geometry variables to be optimised. For the objective function, the parameters were described and the constraints and assumptions were listed.

Chapter 4

Numerical Method

_____

4.1 Introduction

In this chapter, the numerical optimisation method is discussed. The settings used in the algorithm are shown. The method of calculating the derivatives of the objective function in each of its geometry variables is given. Different parameters are considered in the optimisation algorithm. The way in which these parameters are incorporated in the analysis is shown.

4.2 Optimisation algorithm

The maximum net power output for the open and direct solar thermal Brayton cycle can be found by maximising the objective function. The optimisation algorithm finds the optimum geometry for the solar receiver and recuperator at a specific operating condition in the pressure ratio range of a specific micro-turbine so that the net power output of the system can be a maximum. The six geometric variables to be optimised are listed in Table 4.1.

Table 4.1 Geometric variables used in numerical optimisation with description.

Variable	Description	Numerical variable
$D_{h,rec}$	Hydraulic diameter of the cavity receiver channel / tube (m)	$X(1)/100$
L_{rec}	Channel / tube length of the cavity receiver (m)	$X(2)$
a/b_{reg}	Aspect ratio of the recuperator channels	$X(3)$
$D_{h,reg}$	Hydraulic diameter of the recuperator channels (m)	$X(4)/1000$
L_{reg}	Length of the recuperator (m)	$X(5)$
a/b_{rec}	Aspect ratio of the cavity receiver channel / tube	$X(6)$

The vector X will be optimised by the optimisation algorithm. Also take note that some of these variables are scaled to ensure that the variables in the variable vector are more or less of the same order. The objective function (net power output of the system), in terms of the geometry

variables, parameters and constants, is maximised using the dynamic trajectory optimisation method by Snyman (2009). Take note that the optimisation algorithm used (LFOPC by Snyman (2000) or the leapfrog method) requires a function input to be minimised. The objective function (equation 3.61) is multiplied with -1, since the objective function should be maximised (see the function '*fun*' in Appendix C). The minimum of the negative function would then be negative, but when multiplied again with -1, it would give the positive maximum of the objective function (Snyman, 2009). Note that, in Appendix C, the leapfrog method is called using the MATLAB function *lfopc([starting vector])* by Snyman (2000). The following settings in Table 4.2 (mostly the default settings) were used for the dynamic trajectory optimisation algorithm by Snyman (2000).

Table 4.2 Settings used for the optimisation algorithm (LFOPC).

Setting	Definition	Chosen Value
x0	Starting point: this depends on the specific micro-turbine	The starting point for small micro-turbines is [5 5 5 5 5], while the starting point for large micro-turbines is [10 10 10 10 10 10]
delt	Maximum step size	1 (default)
xtol	Convergence tolerance *ex* on the step movement	1e-7 (the default is 1e-8)
eg	Convergence tolerance *eg* on the norm of the gradient	1e-5 (default)
xmu	Initial penalty value	100 (default)
xmumax	Maximum penalty value	10 000 (default)
kmax	Maximum number of steps per phase	1 000 (default)

The results from two other optimisation algorithms from Snyman (2009) were compared with the dynamic trajectory optimisation method: the spherical quadratic steepest descent (SQSD) method for unconstrained minimisation with no explicit line searches and the gradient-only conjugate gradient method for constrained minimisation with no explicit line searches. These optimisation algorithms were not able to find a solution as sound as the dynamic trajectory optimisation method for constrained optimisation.

4.3 Gradients

The optimisation algorithm by Snyman (2000) requires the gradient of the objective function in each variable. As can be understood, to get the gradient of the objective function for each

variable (in this work) is difficult. As a first attempt, the variables of the objective function were written in symbol form so that the 'grad' function in MATLAB could be used to give the equations for these gradients. Such an equation was, unfortunately, pages long and made its handling and copying very difficult. Keep in mind that there is an iteration involved in the objective function (see Section 3.6), which makes the calculation of its slope in a certain variable a very difficult process.

The solution was to go back to the definition of the gradient of a function (Stewart, 2003). The gradient of the function for each of the variables in vector X can be obtained by taking a small increment h positive and negative of the variable value, to get two function values (derivative functions). The slope can then be calculated at the specific point in space. Note that in the following equations, X is the vector containing the variables that should be optimised in the optimisation algorithm. In the function 'gradf' (Appendix C), the following was done to obtain the gradient of the function in a certain variable at a specific point of the vector X:

Let h be very small: $h = 1 \times 10^{-8}$. The gradient $\dfrac{dfun}{dX(1)}$ can then be calculated as:

$$GF(1) = \frac{fun(X+) - fun(X-)}{2h} \qquad (4.1)$$

where '*fun*' is the objective function (see Appendix C) and

$$X+ = X + [h\ 0\ 0\ 0\ 0\ 0] \qquad (4.2)$$

$$X- = X - [h\ 0\ 0\ 0\ 0\ 0] \qquad (4.3)$$

The gradient of the function in the other five variables is calculated similarly. The same method is used for calculating the slopes of inequality constraints as required from the optimisation algorithm. The functions used in the optimisation algorithm are added in Appendix C. The inequality constraints are shown in the function 'conin' and their gradients in each variable are given in the function 'gradc'.

4.4 Structure of the program

Different parameters (D, MT and r) are used in the objective function and different combinations of parameters are considered. A range of parabolic concentrator diameters (D = 6 – 18 m) is used in increments of two metres. For each concentrator diameter, 45 different standard micro-

turbines are considered and for each micro-turbine, the objective function (equation 3.61) is maximised at each of the micro-turbines' operating conditions (from r_{low} to r_{high} in increments of 0.1). The function '*once*' (see Appendix C) is used to do the abovementioned. It is applied in the following summarised structure.

- ➢ Get location-specific constants
- ➢ For **D** = 6 : 2 : 18
    - ○ Get $\dot{Q}_{net}$ from the function '*collector*' (Appendix C), as a function of the receiver geometry variables (or d) according to the receiver sizing algorithm in Appendix A (see Figure A.4). The function '*collector*' calculates the rate of intercepted heat and rate of heat loss for a range of cavity aperture diameters. The receiver sizing algorithm in Appendix A establishes the link between the concentrator size, cavity aperture size and net absorbed heat rate.
    - ○ For all the compressor and turbine pairs from Garrett in Appendix D (*MT* = 1 : 45)
        - ▪ For $r = r_{low}$: 0.1 : r_{high} (along the line of highest compressor efficiency on the compressor map)
            - • Get maximum net power output using the optimisation algorithm and objective function (equation 3.61)
            - • Get optimum geometry variables: $X(1)$, $X(2)$, $X(3)$, $X(4)$, $X(5)$ and $X(6)$
        - ▪ end
    - ○ end
- ➢ end

Figure 4.1 shows how different combinations of concentrator diameters and micro-turbines are considered in the analysis.

Also note that, in the objective function '*fun*', an iteration is performed to establish the temperatures and pressures as discussed in Section 3.6. This iteration continues until the error of the iterations is smaller than 1×10^{-3}. The same method is used in the function '*Tsfunc*' (Appendix C), which calculates the receiver surface temperature. In this function, again, an iteration is performed to determine the temperature, and pressure values to determine the output value of the function.
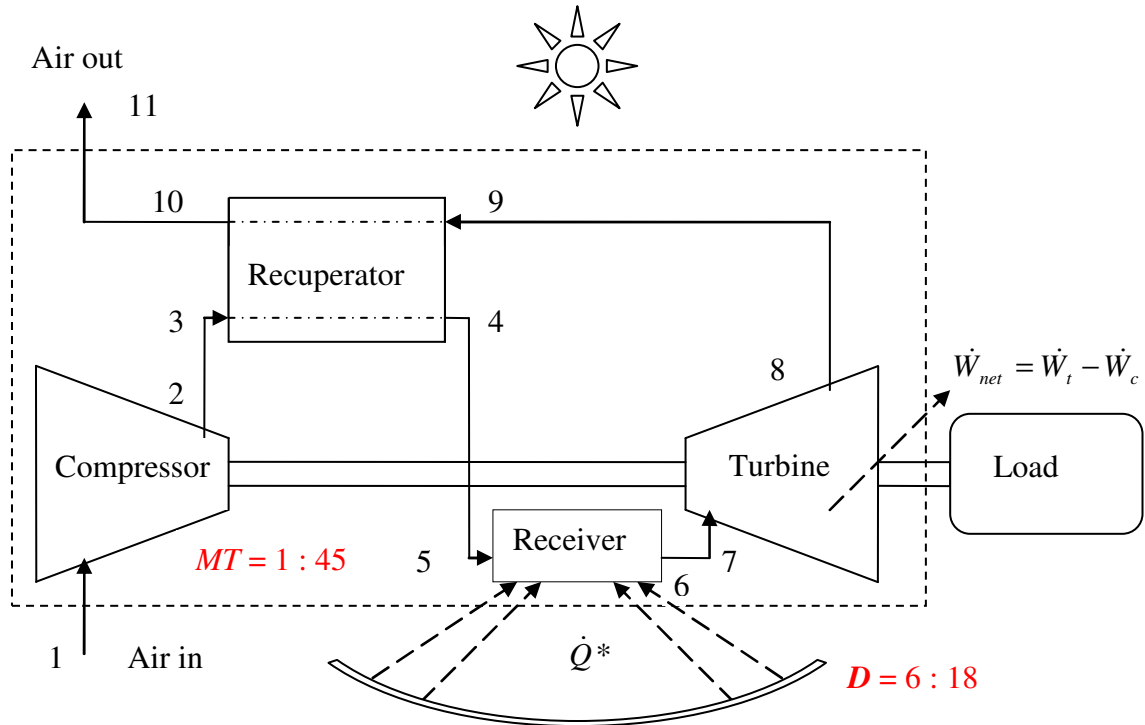
**Figure 4.1 The open and direct solar thermal Brayton cycle with a range of concentrator diameters (D)
and a range of micro-turbines (MT).**

4.5 Summary

The optimisation algorithm used in the analysis is the leapfrog method (LFOPC) by Snyman (2000). The settings used in the analysis for this algorithm were shown in this chapter. The calculation of the derivatives of the objective function was shown. The structure of the analysis and the incorporation of the parameters were highlighted. The results found with the optimisation algorithm (using different parameters) are shown in Chapter 5.